

## **Study of cyclic heat treatment on carbon steel**

**Mahmoud Alasaad\*** and **Wardan Wahhod\*\***

Albaath University, Homs, Syria

\* mmwwq@hotmail.com \*\* ola.nassif@Gmail.com

DOI: <https://doi.org/10.47372/uajnas.2015.n2.a10>

### **Abstract**

In this work, an annealed Ck85 carbon steel was subjected to cyclic heat treatment process that consisted of repeated short-duration (3.4 minutes) holding at 8000C (above Ac3 temperature) followed by forced air cooling. After 8 cycles (about a total 1 hour and 10 minutes duration of heating and cooling cycles), the microstructure mostly contained fine ferrite grains (grain size of 7  $\mu\text{m}$ ) and spheroidized cementite. This microstructure possesses an excellent combination of strength and ductility. The disintegration of lamellae through dissolution of cementite at preferred sites of lamellar faults during short-duration holding above Ac3 temperature, and the generation of defects (lamellar faults) during non-equilibrium forced air cooling were the main reasons of accelerated spheroidization. The strength property initially increased, mainly, due to the presence of finer micro constituents (ferrite and pearlite) and thereafter marginally decreased with the elimination of lamellar pearlite and appearance of cementite spheroids in the microstructure. Accordingly, the fractured surface initially exhibited the regions of wavy lamellar fracture (pearlite regions) along with dimples (ferrite regions). By increasing number of heat treatment cycles, the regions of dimples gradually consumed the entire fractured surface.

**Key words:** Carbon steel, cyclic heat treatment, cementite dissolution, lamellar faults, accelerated spheroidization, mechanical properties.

### **Introduction**

Recent investigations have established the potential of cyclic heat treatment techniques to accelerate several solid state metallurgical processes. Sista et al.[6] applied a cyclic austempering technique to accelerate bainitic transformation in 1080 steel. Sahay et al.[3] found an accelerated grain growth behavior in a cold rolled AlK-grade steel (0.05%C,0.05% Al and 45 ppm N) subjected to cyclic annealing treatment. On the other hand, it has been a challenge for steel industry to accelerate the spheroidization of pearlitic structure, since the conventional spheroidization process of steel, consisting of a subcritical annealing treatment, takes a long time. In an annealed Fe-0.79 wt% C alloy, the spheroidization remains incomplete even after 100 hours of holding at 7000C [7]. In 0.72%C steel with fine pearlitic structure, isothermal annealing at 6800C requires 72hours of holding for nearly 100% spheroidization, whereas with coarse pearlitic structure,50 hours of holding only causes 50% spheroidization [10]. Therefore, in order to accelerate spheroidization, several techniques have been developed such as (a) thermal cycling near Ac1 temperature, (b) isothermal annealing with the aid of prior cold work,(c) hot deformation before, during or after the transformation of austenite to pearlite, and(d) decomposition of supercooled austenite at a temperature slightly below Ac1 [14]. The thermal cycling (swinging annealing) of  $\pm 50\text{C}$  around Ac1 temperature facilitates the dissolution of cementite lamellae when temperature is raised above Ac1. On subsequent cooling below Ac1, this dissolution process is interrupted and the fragmented cementite particles coagulate more easily and quickly [2]. Baranova and Sukhomlin[9] observed that the prior cold working generates defects in the atomic crystal structure of both ferrite and cementite that affects mechanism and kinetics of pearlite spheroidization. Under the influence of previous cold work, during subcritical annealing of steel, the process of cementite separation into pieces is made easier. During subcritical annealing, the cementite in deformed steel is found to disintegrate along slip bands, grain or sub grain boundaries of ferrite. In contrast, Zhu and Zheng [5] studied a direct spheroidization process during hot rolling of hypereutectoid GCr15 steel. The

direct spheroidization is promoted by a combination of low deformation temperature and slows cooling rate that happens to augment the divorced eutectoid transformation reaction. Under such conditions, during phase transformation, carbide particles are likely to grow independently on the pre-existing carbide ‘nuclei’ and result in a poor carbon area to form ferrite. This generates a final microstructure consisting of a ferrite matrix and spheroidized carbide particles. Another method of accelerated spheroidization (known as ‘complete thermal cycling process’) involves austenitizing, followed by rapid quenching to a temperature slightly above the martensite-start transformation temperature ( $M_s$ ), finally up-quenching to a temperature slightly below the  $A_{c1}$  temperature for isothermal annealing. The supercooled austenite possesses large dislocation density and during subcritical annealing just below the  $A_{c1}$  temperature, these dislocations aid the nucleation of cementite particles. This causes a rapid spheroidization through the abnormal decomposition of austenite [14]. Storojeva et al.[8] applied a heavy warm deformation technique for accelerated spheroidization of 0.36 wt% carbon steel and compared the results with conventional subcritical spheroidization process. The heavy warm deformation at 6700C for a total duration of 2 hours produced a microstructure of spheroidized cementite in a fine grained ferrite matrix (grain size = 2  $\mu\text{m}$ ). This provided a good combination of strength and ductility (yield strength = 510 MPa, UTS = 630 MPa, %Elongation = 21). On the other hand, isothermal annealing at 7100C for 16 h produced a microstructure of spheroidized cementite in coarse ferrite matrix along with some amount (30%) of lamellar pearlite that possessed relatively lower strength (yield strength = 340 MPa, UTS = 520 MPa, %Elongation = 29). Kawasaki Steel[10] also utilized the warm deformation process to develop next generation technology for manufacturing electric resistance welded steel tubes (composition: 0.3 wt% C, 0.2 wt% Si, 0.8 wt% Mn). The warm deformation process, with starting temperature above  $A_{c1}$  (7800C) and finishing temperature below  $A_{c1}$  (6700C), produced a spheroidized microstructure possessing adequate strength and excellent formability. The present investigation is an independent approach that applies a cyclic heat treatment process consisting of repeated short-duration holding above the  $A_{c3}$  temperature, followed by forced-air cooling, in order to achieve refinement of the microstructure along with an accelerated spheroidization in a Ck85 carbon steel.

### **Experimental Procedure**

As-received material was a homogenizing annealed Ck85 steel. The homogenizing annealing was carried out at 10000C for a period of 60 minutes. Chemical composition of the steel, analyzed by an optical emission spectrometer (WAS, FMSN: 01G 00 26), is given in Table 1. Annealed steel rods of dimension 65 mm and diameter 5 mm were subjected to cyclic heat treatment for different numbers of cycles, viz. 1-cycle, 3-cycle, 5- cycle and 8-cycle. Each cycle consisted of inserting the specimen in an electric resistance furnace at 8000C (above  $A_{c3}$  temperature, 7600C) and holding for 3.4 min, followed by forced air cooling to the room temperature. The temperature control accuracy of the electric resistance furnace was  $\pm 50\text{C}$ . In each cycle, the air flow rate was maintained at 6 m<sup>3</sup>/h with, a total cooling time of 4 minutes. In order to study the extent of cementite dissolution, one as-received specimen of similar dimension was heated to 8000C, held for 3.4 min and quenched in ice-brine solution. Thereafter, all specimens were sectioned to small pieces and polished with successive grades of emery papers up to 1000 grit size, followed by cloth polishing with 1  $\mu\text{m}$  diamond paste. These specimens were etched by 2% NITAL and examined under metallurgical microscope (Leica, REICHERT, POLYVAR2). The size of ferrite grains was measured as per ASTM E112 standard[9] in the specimen containing significant amount of ferrite with grain boundary clarity (specimen subjected to 8 heat treatment cycles). In order to determine the prior austenitic grain size of the as-received steel, a piece of steel was isothermally held at 10000C for 60 minutes, followed by quenching in water at 400C. The prior austenitic grains were clearly revealed on polishing, followed by 2% NITAL etching, and the grain size was measured as per ASTM E112 standard[9]. The hardness of all the specimens was measured in a Vicker’s hardness testing machine (BIE, BV-250(S)) using 30 Kg load. In order to investigate mechanical

properties, standard tensile test was carried out for as-received and cyclic heat treated specimens with 25 mm gauge length in a servohydraulic universal testing machine (UTE 60) of 600 KN capacity at a crosshead speed of 0.03 mm.s<sup>-1</sup>. Further, the polished and etched metallographic specimens and the fractured surfaces of tensile tested specimens were examined in a Scanning Electron Microscope (Hitachi, S- 3000N) under secondary electron image mode. The sizes of the isolated cementite spheroids were measured (in case of sufficiently spheroidized specimens) from SEM images at high magnification. The size of a spheroid was considered as the average of major axis and minor axis of an approximated ellipse in two-dimension. In order to analyze different phases present, all the specimens were subjected to X-ray diffraction (XRD) analysis with slow scan rate (10/minute) in a high resolution X-ray diffractometer (X'Pert PRO, PANalytical B.V., PW3040/60, The Netherlands).

## **Results and Discussion**

### **Microstructural changes with heat treatment cycles:**

The prior austenitic grain size (Fig.1) of as-received steel on homogenizing annealing at 1000C, with 60 minutes hold, is measured as 147  $\mu\text{m}$ . This is the representative prior austenitic grain size for entire set of experiments. The XRD profiles of the as-received annealed specimen and the specimens subjected to different cyclic heat treatment schedules are presented in Fig.2. All these specimens exhibit the presence of two phases,  $\alpha$ -ferrite and cementite. The morphologies of these phases are revealed in optical and SEM-micrographs. The optical micrographs of the as-received annealed specimen and the specimens subjected to heat treatment for different numbers of cycles are presented in Fig.3(a)-(e). In the annealed specimen, the ferrite phase is present as 'eutectoid ferrite' within pearlite and as proeutectoid ferrite. The cementite phase is present initially only as the 'eutectoid cementite' (lamellar cementite) within pearlite. However, with the increasing number of heat treatment cycles, the amount of lamellar pearlite decreases and the amount of cementite spheroids increases. After 8 cycles, the microstructure mainly contains cementite spheroids and ferrite with trace amount of lamellar pearlite. The SEM secondary electron images of metallographic specimens (Fig.4 & Fig. 5(a)-(g)) corroborate the detail mechanism of spheroidization process. The SEM secondary electron image of the specimen held at 8000C for 3.4 minutes, followed by quenching in ice-brine solution, is shown in Fig.4. The presence of partially dissolved fragmented cementite lamellae indicates that, during short time (3.4 minutes) holding at 8000 C, the dissolution of cementite lamellae in the pearlitic region remains incomplete. This is not unexpected, since in the process of austenitization, the ferrite-to-austenite transformation occurs very fast, whereas the cementite dissolution in austenite is a slow process [12,13]. The SEM secondary electron images of the specimens subjected to heat treatment for different number of cycles are presented in Fig. 5(a)-(g). The SEM image (Fig.5(a)) exhibits fragmented cementite lamellae surrounded by fine pearlitic region and dark ferrite regions in the steel heat treated for single cycle. The fine pearlitic region originates from carbon enriched austenitic regions during forced air cooling. The austenite in proximity to the fragmented cementite region is likely to be enriched with carbon through cementite dissolution; whereas, in the regions away (including prior proeutectoid ferrite region), austenite remains devoid of carbon. The carbon-devoid austenite regions is converted into ferrite upon forced air cooling. The incomplete dissolution of cementite results in the fragmented cementite lamellae that appear in the form of long ribbons, rods and sometimes as relatively thicker irregular shapes after single heat treatment cycle, as shown in Fig.5(a)-(c), while in most of the places fragmented cementite lamellae appear as ribbons or rods (Fig.5(a)-(b)), at few locations thick irregular shapes are found (Fig.5(c)). A real pearlitic lamellar structure is never perfect. The defect enriched lamellar fault regions of higher curvature, such as kinks, striations, holes, fissures and terminations always exist in cementite lamellae. These regions of higher curvature possess higher chemical potential [7]. Therefore, in the present study, these lamellar fault sites act as the sites of higher chemical potential, with respect to both the adjacent austenite and the adjacent flat surface of same lamella. Cementite dissolution preferentially occurs

at the lamellar fault sites through diffusion of atoms to the adjacent austenite from these fault sites. With short holding time (3.4 minutes) at 8000C, the incomplete dissolution of cementite results in the breakdown of cementite lamellae, producing rod and ribbon shaped cementite. On the other hand, the diffusion of atoms from the lamellar fault sites to the adjacent flat surfaces of a cementite lamella causes thickness of lamella. This diffusion process may also have secondary effect on the fragmentation of a cementite lamella through the removal of atoms from fault regions. It is important to note that the main mechanism of conventional subcritical isothermal spheroidization is the atomic diffusion from highly curved lamellar fault sites to the neighboring flat interfaces as explained by 'fault migration theory' [7]. Therefore, in the present study the lamellar breakdown is augmented by another high temperature diffusional process i.e. the diffusion of atoms from lamellar fault sites to the adjacent austenite during austenitization. Furthermore, the non-equilibrium forced air cooling is known to introduce more defects in the structure. Thus, the fine pearlite originated from forced air cooling (non-equilibrium cooling) is likely to possess increased number of lamellar fault sites (defect enriched regions) on cementite lamellae which happens to accelerate the spheroidization process in subsequent heat treatment cycles. This is clearly evident in the secondary electron images of the specimen subjected to 3 heat treatment cycles (Fig. 5(d)-(e)). Several cementite spheroids are generated along the axis of lamellae (Fig. 5(d)) and at terminations of lamellae (Fig. 5(e)). Many spheroids are found to be adhered to the lamellae and isolated spheroids are relatively less. For still higher number of heat treatment cycles (5-cycle), the spheroids tend to grow in size, their adherence to the lamellae is relatively less and their presence is more isolated (Fig. 5(f)). Finally, after 8 cycles of heat treatment, the microstructure mostly contains isolated cementite spheroids and ferrite (Fig.3(e) & Fig.5(g)). The total time required in execution of 8 heat treatment cycles is about 1 hour 10 minutes. The conventional subcritical spheroidization requires much longer time (about 100 hours) [3,4]. Therefore, the present cyclic heat treatment process can be considered as an alternate route of accelerated spheroidization. The rapid spheroidization in the present investigation is mainly attributed to three major factors. Firstly, the process temperature is very high (above Ac3) that makes all diffusional processes faster. Secondly, the incomplete cementite dissolution process augments spheroidization, which is absent in conventional subcritical spheroidization process. Thirdly, in each cycle, the non-equilibrium forced air cooling generates more lamellar faults that act as potential sites for the diffusion assisted spheroidization process.

### **Mechanical properties:**

The variation of hardness and mechanical properties with a number of heat treatment cycles is given in Table 2 and graphically presented in Fig.6. The hardness and strength properties (yield strength and ultimate tensile strength) gradually increase up to 5 cycles and then decrease. The initial increase in hardness and strength properties is due to the finer microstructure (finer pearlite and ferrite) originated from non-equilibrium forced air cooling in each heat treatment cycle. After 8 heat treatment cycles, hardness and strength properties marginally decrease, with respect to that of 5 heat treatment cycles, due to elimination of lamellar pearlite and generation of more cementite spheroids in the microstructure. However, the steel still possesses much higher strength than the asreceived steel due to extremely fine grain size of ferrite in the microstructure. The measured grain size of ferrite matrix, in the specimen subjected to 8 heat treatment cycle is 7  $\mu\text{m}$ . The ductility property (% elongation) initially decreases marginally due to the generation of finer structure and, thereafter, slightly increases with the gradual elimination of lamellar pearlite in the microstructure. The specimen subjected to 8 heat treatment cycles and the as-received homogenizing annealed steel possess same ductility. The measured sizes of the cementite spheroids for the specimens subjected to heat treatment for 5-cycle and 8-cycle are 0.49  $\mu\text{m}$  and 0.53  $\mu\text{m}$ , respectively. These submicron cementite spheroids are much smaller in size than the cementite spheroids generated through conventional isothermal spheroidization process [10]. The cementite spheroids, being very small in size and dispersed in a fine-grained ferrite matrix, do not cause any

reduction in ductility and provide adequate strength. Therefore, in the present study, the cyclic heat treatment process generates a microstructure of spheroidized cementite in fine grained ferrite matrix that provides an excellent combination of strength and ductility (yield strength = 390 MPa, UTS = 727 MPa, %Elongation = 32). Adequate strength is achieved through grain refinement and a reasonable ductility is retained with the presence of spheroidized cementite in the microstructure. A similar microstructure with a good combination of ductility and strength properties was achieved by Storojeva et al.[8]through warm deformation of 0.36 wt% C steel at 6700C for duration of two hours. The other heat treatment processes, such as austempering treatment of bearing steel producing an optimum duplex microstructure of bainite and martensite, have been reported [14] to also provide an excellent combination of hardness, strength and toughness.

### **Fractured surface:**

The SEM secondary electron images of the fractured surfaces of tensile tested specimens are presented in Fig. 7(a)-(e). The fractured surface of as-received steel (Fig.7(a)) exhibits dimples (indicated as 'D') and wavy regions of lamellar fracture (indicated as 'LF'). The dimples are originated from microvoid coalescence, mainly in the ferritic regions. The lamellar fracture is exhibited in the pearlitic region representing crack nucleation and propagation along the junction of different pearlite colonies. The steel subjected to single-cycle heat treatment also exhibits similar nature of fracture (Fig. 7(b)). This has happened so because single cycle heat treatment only causes fragmentation of cementite lamellae (during holding at 8000 C) and generation of fine pearlitic structure (during forced air cooling). In fact, no cementite spheroid appears in the microstructure at this stage. From 3-cycle onwards, when cementite spheroids appear, the proportion of dimples increases and the extent of lamellar fracture decreases (Fig. 7(c)-(e)). The steel, subjected to 3 cycles of heat treatment, exhibits dimples on majority part of the fractured surface (Fig.7(c)). The pearlitic areas (small proportion) appear flat and the wavy lamellar nature is lost. Gradually, the regions of dimple rupture occupy almost the entire fractured surface, as observed in the specimen subjected to 5 heat treatment cycles, whereas only a few locations exhibit flat fractured surface (Fig. 7(d)). Finally, after 8 cycles of heat treatment, almost entire fractured surface is occupied by small dimples (Fig. 7(e)).The microvoid coalescence mode of failure represented by the presence of dimples is in concurrence with the elimination of lamellar pearlite, and the domination of spheroidized cementite and ferrite in the microstructure of the steel subjected to 8 heat treatment cycles.

### **Conclusion**

- (i) The cyclic heat treatment consisting of repeated short-duration holding at 8000C (above Ac3) followed by forced air cooling accelerates the spheroidization process in Ck85 carbon steel.
- (ii) The fragmentation of lamellae is augmented by the dissolution of cementite through atomic diffusion from preferred sites of 'lamellar fault' in cementite to the adjacent austenite during short-duration holding above Ac3 temperature. The non-equilibrium forced air cooling generates more lamellar fault regions that act as the potential sites for spheroidization.
- (iii) With the increasing number of heat treatment cycles, the proportion of ferrite and spheroidized cementite increases, the proportion of lamellar pearlite decreases and microconstituents (pearlite and ferrite) become finer.
- (iv) After 8 heat treatment cycles, the microstructure mostly contains spheroidized cementite particles in very fine ferrite matrix (grain size of 7  $\mu\text{m}$ ) with an excellent combination of strength and ductility properties.
- (v) Initially, the strength property increases mainly due to the presence of finer microconstituents (ferrite and pearlite).Thereafter, it decreases marginally with the elimination of lamellar pearlite and the appearance of cementite spheroids in the microstructure. Accordingly, ductility exhibits marginal decrease and increase with increasing number of heat treatment cycles.
- (vi) The fractured surface initially exhibits the regions of wavy lamellar fracture (pearlite regions) along with dimples (ferrite regions). The regions of dimples gradually consume the entire fractured surface and the areas of lamellar fracture are gradually eliminated with increasing number of heat treatment cycles.

Table 1: Chemical composition of as-received steel (wt.%)

C	Si	Mn	P	S	Cr	Cu	Ni	Al	Fe
0.868	0.19	0.47	0.001	0.001	0.080	0.035	0.030	0.006	Balance

Table 2: Results of tensile test and hardness test

No. of heat treatment	Yield strength (MPa)	Ultimate tensile strength (MPa)	%Elongation	Hardness (HV)
as-received steel(0)	586	756	11.2	262
1	591	847	11.5	270
3	641	910	11.9	279
5	813	1064	12.8	282
8	655	949	12.3	264

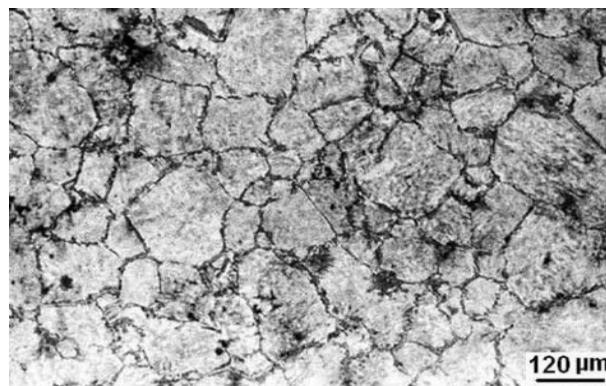


Figure 1: Optical micrograph representing the prior austenitic grain size of as-received annealed steel

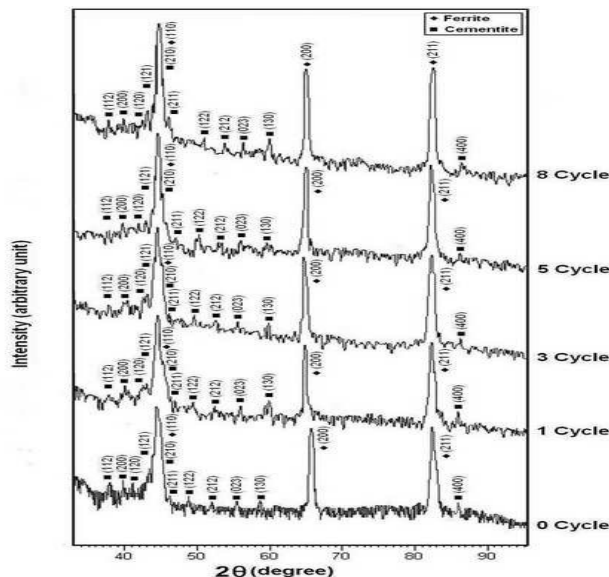


Figure 2: The results of X-ray diffraction study

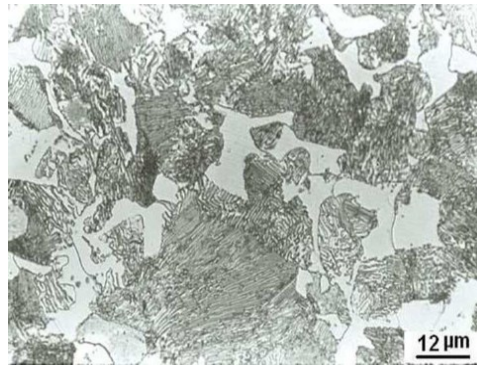


Figure 3: Optical micrographs of the as-received annealed specimen and the specimens subjected to heat treatment for different number of cycles: (a) as-received,

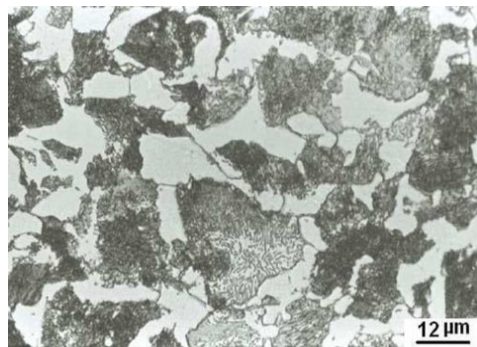


Figure 3: Optical micrographs of the as-received annealed specimen and the specimens subjected to heat treatment for different number of cycles: (b) 1-cycle

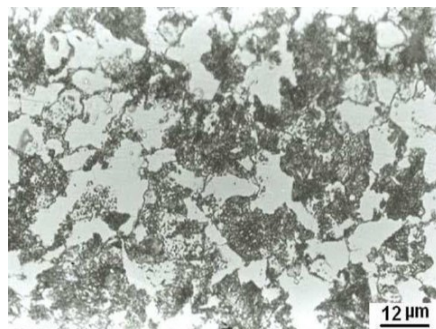


Figure 3: Optical micrographs of the as-received annealed specimen and the specimens subjected to heat treatment for different number of cycles: (c) 3-cycle



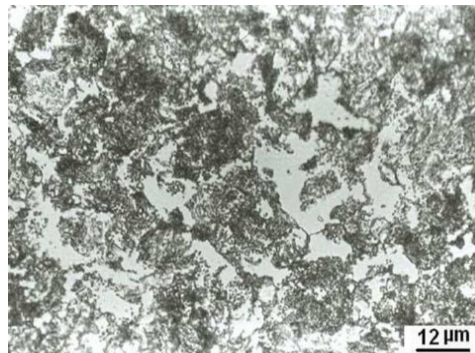


Figure 3: Optical micrographs of the as-received annealed specimen and the specimens subjected to heat treatment for different number of cycles: (d) 5-cycle

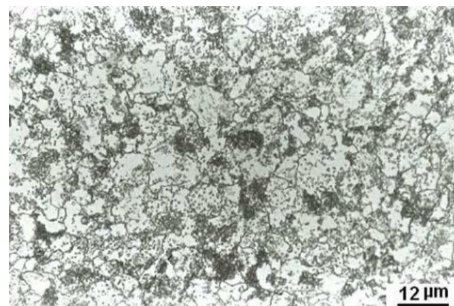


Figure 3: Optical micrographs of the as-received annealed specimen and the specimens subjected to heat treatment for different number of cycles: (e) 8-cycle

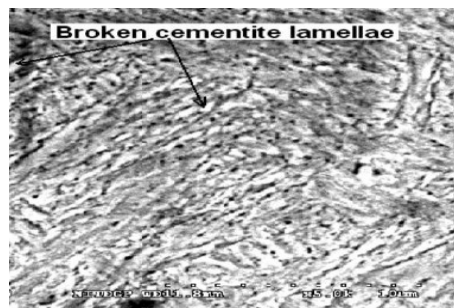


Figure 4: SEM secondary electron image of the specimen quenched from 800°C after holding for 3.4 minutes

Figure 5: SEM secondary electron images of the specimens subjected to different heat treatment cycles:

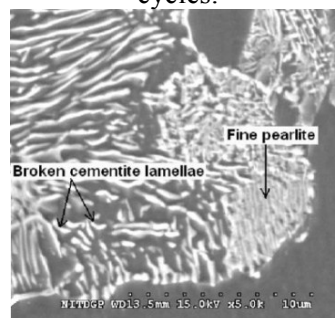


Figure 5(a) 1-cycle: fragmented cementite (rod and ribbon shaped) and fine pearlite,



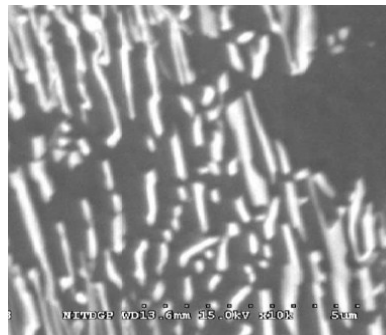


Figure 5(b) 1-cycle: fragmented cementite (rod shaped) at higher magnification

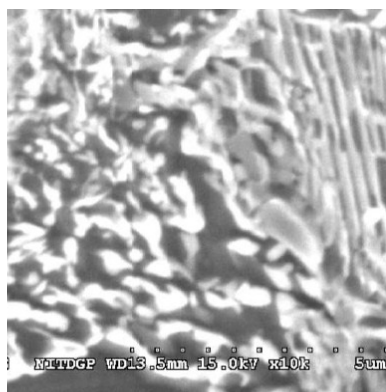


Figure 5(c) 1-cycle: fragmented cementite (thick irregular shaped) at higher magnification

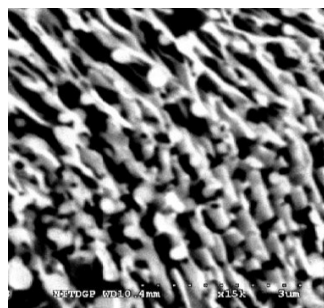


Figure 5(d) 3-cycle: formation of spheroids along the axis of lamellae

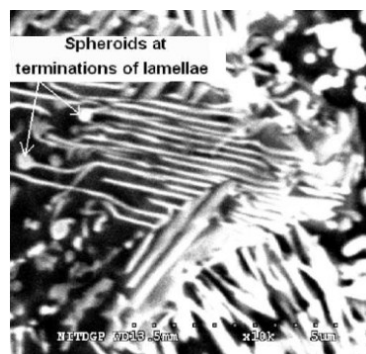


Figure 5(e) 3-cycle: formation of spheroids at the terminations of lamellae

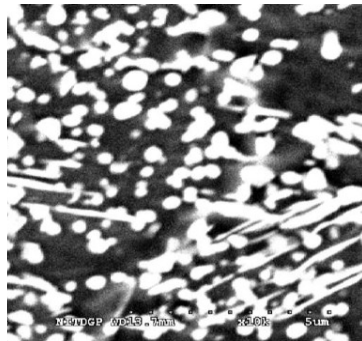


Figure 5(f) 5-cycle

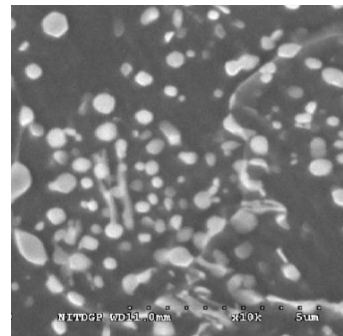


Figure 5 (g) 8-cycle

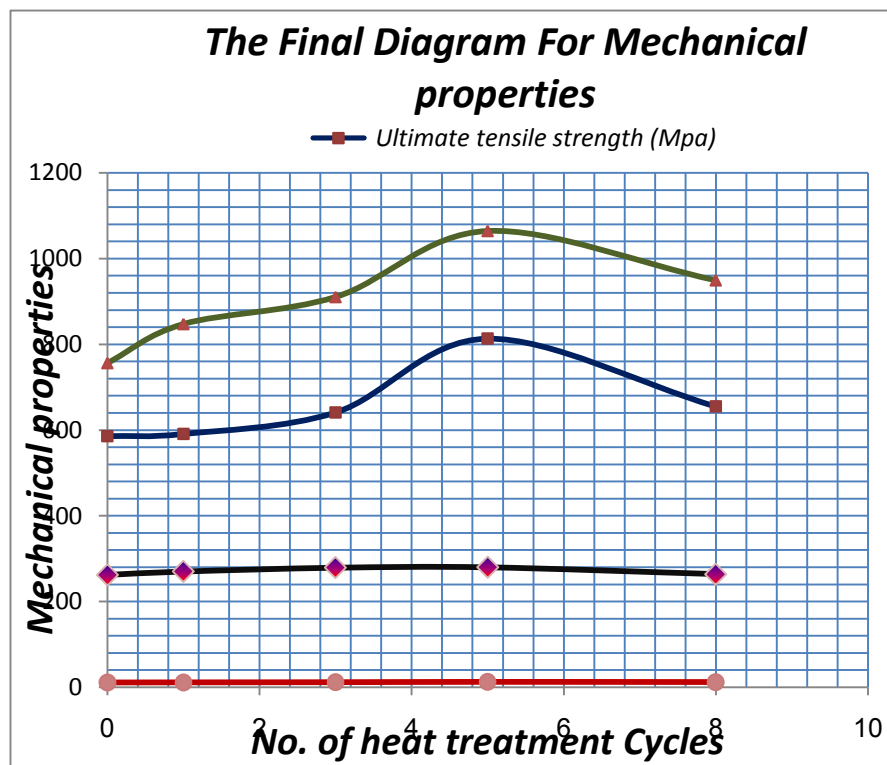


Figure 6: Variation of hardness and mechanical properties with number of heat treatment cycles

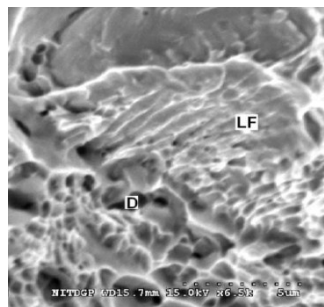


Figure 7: Fractured surfaces of the tensile tested specimens: (a) as-received

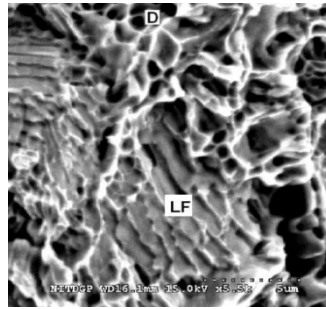


Figure 7: Fractured surfaces of the tensile tested specimens: (b) 1-cycle

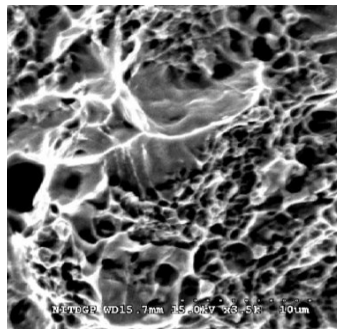


Figure 7: Fractured surfaces of the tensile tested specimens: (c) 3-cycle

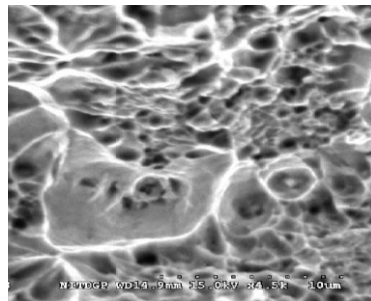


Figure 7: Fractured surfaces of the tensile tested specimens: (d) 5-cycle

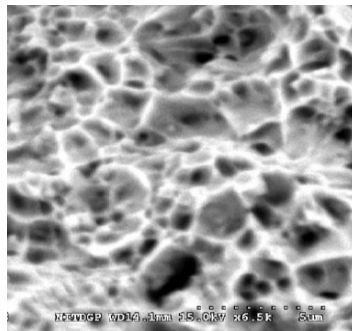


Figure 7: Fractured surfaces of the tensile tested specimens: (e) 8-cycle

**References:**

1. Baranova. V.A and Sukhomlin. G.D, (1981). Spheroidization of cementite in steel - Springer, *Metallovedenie i Termicheskaya rabotka Metallov*.11, (51-55).
2. Chakraborty. J, Bhattacharjee. D and Manna. I, (2008). Development of ultrafine bainite & martensite duplex microstructure in SAE 52100 bearing steel by prior cold deformation, *Scripta Materialia*. 59, ( 247-250).
3. Chou. C.C, Kao. P.W and Cheng. G.H, (1986). accelerate bainitic transformation in 1080 steel, *Mater. J. Sci.* 21 , (3339-3344).
4. Kawabata. Y, Okabe. T and Koyama. Y, (2001). Development of High Carbon HISTORY Steel Tube with Excellent Formability, *Kawasaki Steel Giho*. 33, (155-158).
5. Kumar.R, (1968). *Physical Metallurgy of Iron and Steel*, Asia Publishing House, Bombay, (92 - 93).
6. Liscic. B, (1997). *Steel Heat Treatment Hand Book*, New York, (596).
7. Mondal. D.K and Dey .R.M, (1984). Effect of grain size on the microstructure and mechanical properties of a C-Mn-V dual-phase steel, *Transactions of IIM*. 37, (351–356).
8. Sahay. S.S, Malhotra. C.P and Kolkhede. A.M, (2003). Accelerated grain growth behavior during cyclic annealing , *Acta Materialia*. 51, (339-346).
9. Sista. V, Nash. P and Sahay. S.S, (2007) . Accelerated bainitic transformation during cyclic austempering , *Mater. J.Sci.* 42, (9112–9115).
10. Speich. G.R and Szirmae. A, (1969). *Transactions of the Metallurgical Society of AIME*. 245, (1063–1074).
11. Storojeva. L, Kaspar. R and Ponge. D, (2004). Effects of Heavy Warm Deformation on Microstructure and Mechanical Properties of a Medium Carbon Ferritic-Pearlitic Steel, *ISIJ international*. 44, (1211-1216).
12. Tian .Y.L and Kraft. R.W, (1987). Mechanisms of pearlite spheroidization, *Metallurgical Transactions A*. 18A, (1403–1414).
13. Xie. Xiwen, (1997).*Steel Heat Treatment Hand Book*, New York, (995).
14. Zhu. G and Zheng. G, (2008).directly spheroidizing during hot deformation in GCr15 steels, *Mater. Front. Sci. China*. 2, (72-75).

## دراسة المعالجة الحرارية الدورية على الفولاذ الكربوني

محمود الأسعد و وردان وحود

جامعة البعث - حمص - سوريا

Email: mmwwq@hotmail.com, Email: Ola.nassif@Gmail.com

DOI: <https://doi.org/10.47372/uajnas.2015.n2.a10>

### المخلص

في هذا العمل أُخضع الفولاذ الكربوني الملدن CK85 لعملية المعالجة الحرارية الدورية و المتكونة من فترات قصيرة متكررة (3.4 دقائق) تثبيت عند الـ 800 (فوق حرارة Ac3) مُتبعة بهواء بارد مضغوط. بعد 8 دورات (مدة إجمالية حوالي ساعة وعشرة دقائق لدورات التسخين و التبريد) والبنية على الغالب تحوي حبيبات فريت ناعمة (حجم الحبة 7 ميكرومتر) و سمنتيت متكور. هذه البنية تمتلك تجمع ممتاز من المتانة وقابلية الطرق. تفكك (تكسر) الصفائح من خلال انحلال السمنتيت عند المواقع المميزة من العيوب الصفائحية خلال تثبيت عند الـ 800 (فوق حرارة Ac3) وتتولد العيوب (العيوب الصفائحية) خلال عدم توازن تدفق الهواء البارد كانت الأسباب الرئيسية للتكور بشكل سريع. بدايةً خاصية المتانة تزداد بسبب وجود البنية الناعمة (فريت وبرليت) وتنقص بشكل طفيف فيما بعد مع زوال البرليت الصفائحي وظهور السمنتيت الكروي في البنية. ووفقاً لهذا فإن سطح الانكسار الأولي يظهر مناطق من التكسر الصفائحي المتموج (مناطق برليتية) مع ندبات - غمازات - (مناطق فريتية). ومع تصاعد عدد دورات المعالجة الحرارية فإن مناطق الندبات ستستهلك تدريجياً كامل محيط السطح المكسور.

**الكلمات المفتاحية:** الفولاذ الكربوني، المعالجة الحرارية الدورية، انحلال السمنتيت، عيوب الصفائح، التكور المتسارع، الخواص الميكانيكية.